

Tunable high-frequency band-stop magnetic filters

Bijoy Kuanr, Z. Celinski,^{a)} and R. E. Camley

*Center for Magnetism and Magnetic Nanostructures, Department of Physics,
University of Colorado at Colorado Springs, Colorado Springs, Colorado 80933-7150*

(Received 22 July 2003; accepted 16 September 2003)

We present results on Fe- and PermalloyTM-based microstrip microwave band-stop filters. These structures, prepared on GaAs substrates, are compatible in size and growth process with on-chip high-frequency electronics. We observed power attenuation of 100 dB/cm for Permalloy and 180 dB/cm for Fe. The insertion loss is low: 2–3 dB for Permalloy and 3–5 dB for the Fe-based structures. Our geometry includes a significant boost to the zero-field operational frequency due to the shape anisotropy of the magnetic element in the microstrip. Using the shape anisotropy, we create a Fe-based filter that operates at 11 GHz with zero applied field. © 2003 American Institute of Physics. [DOI: 10.1063/1.1625424]

The frequency range of 10 to 100 GHz is particularly interesting for communications, military, and security applications. For example, there are obvious needs to see through fog, clouds, and smoke, but this cannot be done in visible light or infrared radiation. These obstacles are transparent, however, for electromagnetic waves at particular frequencies in the gigahertz range. Thus, signal processing in this range is of significant importance.

There are a few devices that operate at high frequencies; however, they are large and bulky. Recently we have witnessed incredible progress in high-frequency semiconductor electronics and a movement towards the synthesis of different electronic components into integrated circuits. Here, we describe on-wafer, magnetic devices which are small and could be integrated with high frequency electronics. Reduction of device dimensions in these monolithic microwave integrated circuits is important from the cost and reliability point of view.

The operational frequency f can be obtained from the ferromagnetic resonance condition and is set by material properties, such as saturation magnetization M_s , anisotropy fields H_a , the gyromagnetic ratio γ , and the magnitude of an applied field H . If the applied field is along the easy axis, the frequency is given by

$$f = \gamma \sqrt{(H + H_a)(H + H_a + 4\pi M_s)}, \quad (1)$$

and therefore the resonance frequency can be varied with an external magnetic field.

Most current devices are based on a low-magnetization ferrimagnetic insulator (YIG). Our work, in contrast, uses an approach in which high magnetization, metallic ferromagnets are the active element in these filters. This high magnetization allows the high-frequency operation. Table I shows theoretical results for operational frequencies for different materials. With YIG, an applied field of over 11 kG is necessary to reach frequencies of about 35 GHz. Such large fields are incompatible with devices of a limited size since substantial electromagnets are required. Clearly the use of metallic fer-

romagnets would significantly increase the operational frequency.

While Fe has a much higher resonance frequency for the same applied field, its conductivity can lead to high loss at microwave frequencies. However, structures utilizing thin Fe films minimize conduction loss while still producing high attenuation at the band-stop frequency.^{1,2} Early attempts at producing Fe-film-based structures have succeeded in making filters with high band-stop frequencies and low broadband loss.^{1–3} However, the maximum attenuation only reached about 4–5 dB/cm. Currently, a number of different approaches have been investigated using ferromagnetic metals.^{4–9}

Our theoretical calculations^{10–12} indicated that attenuation in the notch filters was inversely proportional to the thickness of the waveguide. Essentially as one reduces the thickness of the dielectric, a larger fraction of the electromagnetic energy density is contained in the ferromagnetic metal. At resonance, this energy is easily dissipated and one obtains a larger attenuation. Based on this work, we have recently constructed microstrip band-stop filters using a different geometry and growth method, resulting in much higher attenuation.^{4–6} Most of the previous devices have been fabricated using molecular-beam epitaxy (MBE). In contrast, we have constructed magnetic devices grown by magnetron sputtering, a technique commonly used in industry. The sputtering technique has a second advantage. MBE-grown films are generally thin, less than 100 nm, but the microwave devices require thicker films, 1–2 μm , to be on the order of the skin depth in the magnetic material. The sputtering technique is quite capable of producing these thicker films.

Here, we report results on microstrip devices that exhibit

TABLE I. Comparison of operational frequencies for different magnetic materials (assumes $H_a = 0.6$ kG for Fe).

Material	$4\pi M_s$ (kG)	Frequency (GHz) at 1 kG applied field
YIG	1.75	4.8
Permalloy	10.0	9.7
Fe	21.5	17.2

^{a)}Electronic mail: zcelinsk@uccs.edu

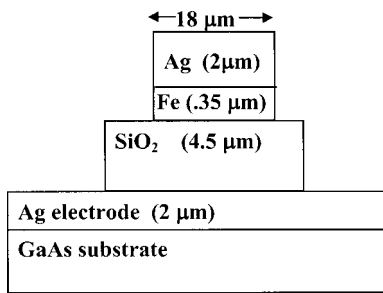


FIG. 1. Structure of the microstrip notch filter.

strong attenuation (up to 180 dB/cm in power measurements) and low insertion loss (2–3 dB). This is accomplished by creating devices with good impedance matching, which is achieved by making the width of the upper microstrip line much narrower: 18 μm (see Fig. 1). Because the upper line includes the ferromagnetic material, there is a second major effect, a boosting of the operational frequency due to the created shape anisotropy in the magnetic material.

In Fig. 1, we show a cross section of our device. Using sputtering, we deposit the following sequence of materials on

GaAs substrates. We begin by growing the bottom electrode: a 2 nm seed layer of Fe, a 2- μm -thick Ag layer, and a Ti layer for adhesion. The rest of the structure is grown through a shadow mask, starting with a 4- μm -thick SiO_2 film, a thin Ti film for adhesion, Fe or Permalloy film (0.3 to 0.5 μm thick), followed by a thick Ag film (1.5 μm thick). The device is patterned by photolithography and dry etched.

We determine the performance of our devices using a vector network analyzer. We characterized the microstrip transmission lines at frequencies from 1 to 45 GHz using an automated vector network analyzer. To remove the influence of cables, probes, etc., an on-wafer calibration was done using the NIST Multical[®] software for the through-open-line calibration procedure.¹³

Before we present our results, we estimate the effect of the shape anisotropy on the operational frequency. The magnetic material in our structure is in the form of a long ribbon with the following dimensions: length=3 mm, width = 18 μm , and thickness=0.35 μm . This leads to the following dynamic demagnetizing factors:¹⁴ $N_x=0.966$, $N_y=0.034$, and $N_z=0$. The formula for the resonance condition is now given by

$$f = \gamma \sqrt{(H + H_a + (N_y - N_z)4\pi M_s)(H + H_a + (N_x - N_z)4\pi M_s)}. \quad (2)$$

If we calculate the frequency at zero applied field, we find that without the shape anisotropy, the frequency is zero (if $H_a=0$). With the shape anisotropy the frequency is about 11 GHz for the Fe structure and about 5 GHz for Permalloy. This is a substantial boost in operational frequency.

In Fig. 2, we plot transmission as a function of frequency for the Py-based microstrips. We first note that the zero-field frequency is slightly above 4 GHz, in reasonable agreement with the previous estimate based on shape anisotropy. The insertion loss over most of the region is on the order of 2–3 dB, while the power attenuation is close to values of 100 dB/cm. The width of the attenuation dip (measured at 3 dB above the minimum, i.e., half-maximum) becomes distinctly

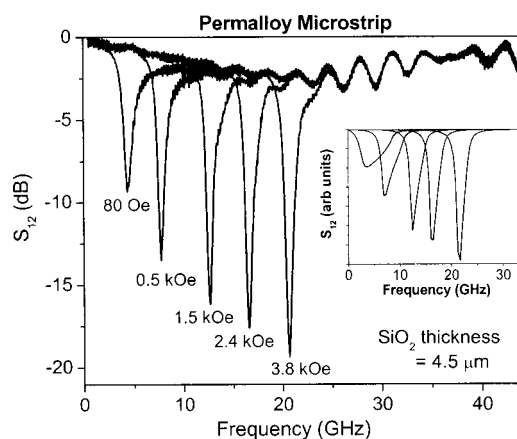


FIG. 2. Transmission parameter in the Permalloy-based notch filter as a function of frequency for different applied magnetic fields. Inset shows theoretical results.

narrower at higher frequencies (0.4 GHz for the dip at 20 GHz compared to a width of 0.82 GHz at 4.3 GHz). This narrowing of the width of the attenuation peak is consistent with our theoretical results as seen in the inset.

In Fig. 3, we show the results for an Fe-based microstrip. The zero-field frequency of about 11 GHz is in excellent agreement with the calculation based on shape anisotropy. For the Fe-based structure, the insertion loss is somewhat larger, between 3 and 5 dB. The power attenuation is dramatically larger: 180 dB/cm at 30 GHz. Again, we see a narrowing of the width of the attenuation dip: it is 3 GHz at 11 GHz and narrows to 1.9 GHz at 30 GHz.

We show the dependence of the operational frequency on applied field in Fig. 4. The dots represent the experimen-

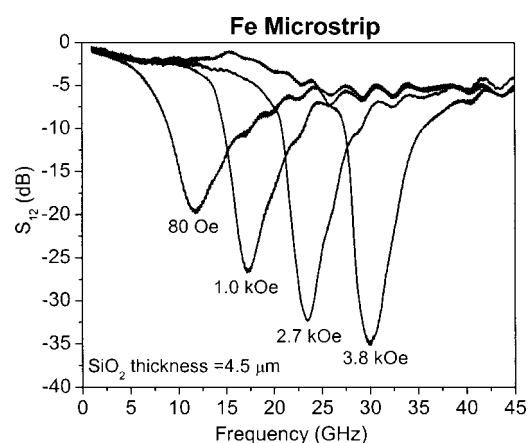


FIG. 3. Transmission parameter in the Fe-based notch filter as a function of frequency for different applied magnetic fields.

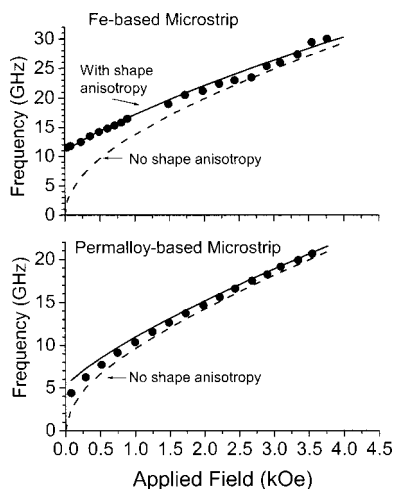


FIG. 4. Frequency of attenuation dip as a function of applied field for Fe and Permalloy notch filters. Note the shape anisotropy produces a significant difference at low fields.

tal results and the solid lines are the theoretical results based on Eq. (2) with no adjustable parameters. The dashed line represents the theoretical results in the absence of shape anisotropy. The effect of the shape anisotropy is clearly present in the experimental data, particularly at low magnetic fields. The effect is substantially larger in Fe than in Permalloy because the saturation magnetization in Fe is more than double that of Permalloy.

In summary, we have designed and built a microstrip notch filter based on ferromagnetic metals. These devices

show large attenuations with relatively low insertion loss. The growth and structuring of the filter is compatible with placing such a device on a chip with additional high-frequency electronics. We also show that substantial increases in operational frequency can be achieved by using shape anisotropy of the ferromagnetic metal.

We acknowledge support from US Army Research Office under grants DAAD19-02-1-0174 and DAAD19-00-1-0146 and from AFOSR project 453-6901 administered by NISSC.

- ¹E. Schloemann, R. Tustison, J. Weissman, H. J. Van Hook, and T. Varitimos, *J. Appl. Phys.* **63**, 3140 (1988).
- ²V. S. Liao, T. Wong, W. Stacey, S. Ali, and E. Schloemann, *IEEE MTT-S Int. Microwave Symp. Dig.* **3**, 957 (1991).
- ³C. S. Tsai, J. Su, and C. C. Lee, *IEEE Trans. Magn.* **35**, 3178 (1999).
- ⁴N. Cramer, D. Lucic, R. E. Camley, and Z. Celinski, *J. Appl. Phys.* **87**, 6911 (2000).
- ⁵N. Cramer, D. Lucic, D. K. Walker, R. E. Camley, and Z. Celinski, *IEEE Trans. Magn.* **37**, 2392 (2001).
- ⁶Bijoy Kuanr, L. Malkinski, R. E. Camley, Z. Celinski, and P. Kabos, *J. Appl. Phys.* **93**, 8591 (2003).
- ⁷E. Salahun, P. Quéffelec, G. Tanné, A.-L. Adenot, and O. Acher, *J. Appl. Phys.* **91**, 5449 (2002).
- ⁸I. Hunyen, G. Goglio, D. Vanhoenacker, and A. Vander Vorst, *IEEE Microwave Guid. Wave Lett.* **9**, 1051 (1999).
- ⁹Y. Zhuang, B. Rejaei, E. Boellaard, M. Vroubel, and J. N. Burghartz, *IEEE Microwave Wireless Components Lett.* **12**, 1531 (2002).
- ¹⁰R. E. Camley and D. L. Mills, *J. Appl. Phys.* **82**, 3058 (1997).
- ¹¹R. J. Astalos and R. E. Camley, *J. Appl. Phys.* **83**, 3744 (1998).
- ¹²R. J. Astalos and R. E. Camley, *Phys. Rev. B* **58**, 8646 (1988).
- ¹³Roger B. Marks, *IEEE Trans. Microwave Theory Tech.* **39**, 1205 (1991).
- ¹⁴A. Aharoni, *J. Appl. Phys.* **83**, 3432 (1998).